Eng. Sci., 2022, **19**, 175–185

Engineered Science

DOI: https://dx.doi.org/10.30919/es8d700

In Vivo Performance of Microstructured Bacterial Cellulose-Silk Sericin Wound Dressing: Effects on Fibrosis and Scar Formation

Biaou O. Ode Boni,[1] Lallepak Lamboni,[1, 2,*] Lin Mao,[1] Bianza M. Bakadia,[1] Zhijun Shi[1] and Guang Yang[1,*]

Abstract

Bacterial cellulose-silk sericin (BC-SS) biomaterials enhance the *in vitro* proliferation of skin cells, forecasting an ability to accelerate wound healing. In a previous study, fibroblasts aligned along the stripes of microstructured BC-SS (mBC-SS), whereas randomly distributed on smooth BC-SS (rBC-SS). Therefore, we hypothesized that *in vivo*, collagens produced by fibroblasts and pivotal for wound contraction could follow the alignment of these cells, which would prevent excessive fibrosis and scaring. The current work reports the *in vivo* evaluation of rBC-SS2 and mBC-SS2 in full-thickness wounds. Overall, improved healing rates were obtained with the composites than with pure BC. Especially, mBC-SS2 induced complete wound closure with hair growth at day 14. Early infiltration of inflammatory cells, fibroblasts, and keratinocytes with the composites led to faster re-epithelialization, vascularization, and wound contraction. Interestingly, mBC-SS2 prevented the excessive wound contraction responsible for hypertrophied neo-tissue formation upon application of rBC-SS2, enhancing healing while containing fibrosis and scar formation.

Keywords: Bacterial cellulose-silk sericin biomaterials; Wound dressings; Re-epithelialization; Wound contraction; Fibrosis; *in vivo*.

Received: 04 July 2022; Revised: 19 August 2022; Accepted: 30 August 2022.

Article type: Research article.

1. Introduction

Bacterial cellulose (BC), a natural polymer produced by some bacteria including *Acetobacter xylinum*, has become very attractive in biomedical applications in the last decade due to its properties.[1] Specifically, due to its mechanical strength and flexibility, BC constitutes a potential biomaterial for wound dressing design.[2–5] Moreover, BC exhibits high crystallinity and a porous structure capable of uptaking wound exudate and maintaining wound site moisture; however, it lacks important bioactivities for tissue engineering such as the mitogenic ability, antioxidant and anti-inflammatory properties, which limits its wound healing abilities.[6] Nowadays, research studies focus on improving the properties of BC with anti-bacterial and/or other bioactivities in order to make it more attractive for wound healing applications.[7–10] Therefore, polymers that naturally exhibit such properties have been combined with BC to prepare composites with novel and improved properties.[11,12]

Silk sericin (SS), another natural polymer produced mainly by silkworms, exhibits interesting bioactivities.[13–16] Several studies have investigated and demonstrated the ability of SS to induce rapid wound healing, which is believed to be due to its biological properties.[17–19] However, SS is brittle in nature and lacks mechanical stability, which limits its application as a wound dressing.[20,21] Therefore, BC-SS composite with a smooth surface (random BC-SS) was designed as a wound dressing in our previous study to take advantage of both their properties. The composite was shown (*in vitro*) to improve the proliferation of fibroblasts, and epithelial cells, pointing out the potential in improving wound healing.[22]

Fibroblasts are the main component cells of the skin dermis,[23] and are responsible for the synthesis of collagen, the extracellular matrix (ECM) which confers strength and elasticity to skin tissue.[24] Thus, during wound healing, the proliferation and differentiation of fibroblasts determine collagen expression, which in turn regulates the healing result with regard to fibrosis and scar formation. In fact, when the proliferation of fibroblasts is not controlled, this can lead to anarchic deposition of collagen[25] responsible for excessive

[1] *National Engineering Research Center for Nano-Medicine, Department of Biomedical Engineering, College of Life Science and Technology, Huazhong University of Science and Technology, 1037 Luoyu Road, Wuhan, 430074, P.R. China.*

[2] *Laboratoire de Biologie Moléculaire et Virologie, Institut National d'Hygiène-Togo, 26 Rue Nangbéto, Quartier Administratif- PO. Box 1396, Lomé-Togo.*

* *Email:* lallepak@yahoo.fr (L. Lamboni)

fibrosis and scarring as we concluded in our recent study.[26] In an attempt of averting such an outcome, we designed the surface of the BC to possess microstructures that can control the distribution and alignment of fibroblasts.[27] Further *in vitro* comparative study of rBC-SS and the microstructured BC-SS (mBC-SS) showed that additionally to displaying the bioactivity necessary for improving cell proliferation, mBC-SS presents good mechanical properties with the ability to induce an ordered alignment of fibroblasts.[26] In this report, we present *in vivo* studies required to assess the wound healing profile resulting from the proposed dressings, including the healing time, the thickness of the new tissue formed, the infiltration of inflammatory cells, the distribution of fibroblasts, and the deposition of collagen to invalidate or confirm the potential of mBC-SS to inhibiting fibrosis and scar formation. Furthermore, the *in vivo* effects of mBC-SS on re-epithelialization, angiogenesis, and wound contraction was evaluated.

2. Materials and methods

2.1 Preparation of samples

Samples were prepared according to the methodology described in our previous studies.[22,26,27] Briefly, to prepare BC, *Acetobacter xylinum* was inoculated in Hestrin & Schramm medium which was composed of citric acid (0.15%, w/v), disodium hydrogen phosphate dodecahydrate (0.68%, w/v), yeast extract (0.5%, w/v), peptone (0.5%, w/v), and glucose (2%, w/v). To obtain BC membranes with the microstructured surface, poly(dimethylsiloxane) (PDMS) with 10 µm width of microgrooves was deposited on the media in order to print its structure on the surface of synthesized BC (mBC) while the smooth surface of PDMS was suspended on the media to generate rBC. After 5 to 7 days of incubation, BC was harvested after having reached 1 to 2 mm thickness, purified, and stored at 4 °C until used.

SS was also extracted according to a procedure previously described.[22] *Bombyx mori* cocoons were cut into small pieces and boiled under pressure in pure water at 120 °C for 1 hour. The SS solution was separated from silk fibroin by filtration and then dialyzed for a concentrate which was then lyophilized, yielding SS powder which was stored at -20 °C until use. To obtain BC-SS composites, priorly sterilized BC was soaked in the SS solution of required concentration (1%, 2%) for 24 hours; then the composites, namely BC-SS1 (rBC-SS1 and mBC-SS1) and BC-SS2 (rBC-SS2 and mBC-SS2), respectively were rinsed with PBS to remove excess SS.[22] The composites were stored at 4 °C and used within one week of their preparation.

According to the results of *in vitro* studies[26] where BC-SS2 released optimum amounts of SS to improve wound healing parameters, mBC-SS2 and rBC-SS2 were selected for *in vivo* comparison of their effects on wound healing, with a focus on the microstructures imparted to BC. Moreover, mBC-SS1 was prepared to assess the influence of SS concentration.

2.2 Animal experimentation

In vivo tests were performed on adult male Wistar rats with the approval of the ethics committee on animal experimentation at Wuhan Xavier Biotechnology Co., Ltd Laboratory. The animals were housed individually in cages kept at 22 ± 2 °C and 60-70% humidity, under cycles of 12 hours light-12 hours dark, while being provided suitable food and water at libidum, with good hygiene conditions. Sixteen adult male Wistar rats at 7-8 weeks and of 200-300 g weight were randomly divided into four groups to be used at different time points including day (D) 3, D7, D14, and D21. The rats were anesthetized with 10% chloral hydrate (abdominal cavity injection), the volume of which depended on animal weight (0.3 mL/100 g). After anesthesia, the dorsal part of the animal was totally shaved and cleaned with alcohol, and six wounds of circular shape 9 mm in diameter were created. The latter were divided into two groups of three wounds per line and separated by the medium line of the dorsal region. The wounds were of full thickness, with a depth covering the epidermis, dermis, and hypodermis. All six wounds were treated with different dressings including mBC, mBC-SS1, mBC-SS2, rBC, rBC-SS2, and gauze as control. The microstructured surface of mBC and its composites was applied against the wound, whereas for rBC and its composites, the smooth surface was the one in contact with the wound. Based on the preliminary assessment (7 days experiment), the dressings were changed every 48 hours during the first 7 days whereas they were changed every 24 hours for the rest of the experiment. At each time point of the test (D3, D7, D14, and D21), macroscopic and microscopic analyses were carried out on three different rats of each group.

2.2.1 Macroscopic Analysis

Wound healing was macroscopically observed at D3, D7, D14, and D21 after surgery. Photographs of the wounds were taken at each time point to appreciate the evolution of wound healing. To determine the healing rate, the wounded area was measured with Image J software (1.51 j8; Java1.8.0_112) and the following Equation (1) was used to calculate the healing rate:

$$HR = \frac{Ao - An}{Ao} \quad (1)$$

HR is the healing rate; A_o and A_n correspond to the wound area at 0 and n days, respectively.

2.2.2 Histological analysis

At each time point, wound tissues were harvested, fixed with 10% formaldehyde, and embedded in paraffin. The tissue samples were sectioned and stained with hematoxylin and eosin (H&E) or Masson trichrome. The stained samples were observed under Pannoramic Scanner to determine the rate of inflammatory cell infiltration, neovascularization, quality of tissue granulation, organization of fibroblast architecture, density, and arrangement of collagen deposition. The thicknesses of tissue granulation and regenerated epidermis were determined by randomly evaluating 10 areas (for each micrograph) while the collagen volume fraction was calculated according to Equation (2) using Image J software.

$$Cv = \frac{Ca \times 100}{Ta} \quad (2)$$

Cv is the collagen volume fraction; Ca and Ta correspond to collagen area and total tissue area respectively.

2.2.3 Immunohistochemical staining

For immunohistochemical staining, the tissue sections were dewaxed with a series of xylene and alcohol solutions and washed with distilled water before being treated with ethylene diamine tetra-acetic acid (EDTA) antigen retrieval buffer (pH 8.0). The tissue sections were then incubated with 10% goat serum for 1 hour at 37 ℃ to avoid non-specific binding, followed by incubation with primary antibodies overnight at 4 ℃, and then with secondary antibodies for 2 hours at 37 ℃. The primary antibodies were those directed against cytokeratin 14 (CK-14, GB11803, dilution 1: 200), vascular endothelial growth factor (VEGF, GB13034, dilution 1: 200), alpha-smooth muscle actin (α-SMA, GB111364, dilution 1:200), collagen I (Col-I, GB11022-3, dilution 1:500), and collagen III (Col-III, GB111629, dilution 1:500), while the secondary antibody was CY3 goat anti-rabbit (GB21303, dilution 1:300). Finally, counterstaining with DAPI was performed for 10 minutes at room temperature in the dark. All reagents were obtained from service (China, Wuhan) and the stained samples were observed under Pannoramic Scanner. The expression rate of different markers was calculated according to Equation (3) using Image J software.

$$Me = \frac{ma \times 100}{Ta} \quad (3)$$

Me is the marker expression rate; ma and Ta correspond to marker area and total tissue area respectively.

2.3 Statistical analysis

One-way analysis of variance (ANOVA) was used with Tukey's multiple comparisons to compare different experimental groups. All statistical analyses were performed with Origin Pro 8 software. Statistical significance was obtained at $P < 0.05$.

3. Results and discussion

The physicochemical properties of the different samples were tested and reported in our previous *in vitro* studies.[26,27] Briefly, it was shown by scanning electron microscope that rBC exhibits random fiber distribution and low-density fiber network with interconnecting pores while at its surface, mBC presents microgrooves with denser, more compact and well-aligned fibers which mimic the microstructure of PDMS templates used during BC production.[26] Moreover, the structure of mBC confers improved mechanical strength to the biomaterial compared to rBC.[27] Further, SS integrated the BC network without modifying its surface structure or crystallinity, though due to its amorphous nature, SS slightly affected the mechanical strength of BC; however, the mechanical properties of the composites remained within the required range for a wound dressing.[22] It was also demonstrated that due to its hydrophilic property, SS improves the moisture retention ability of BC[28] which is of great importance for cleaning necrotic tissue debris, and exudates, and for keeping the wound moist in order to avoid pain and enhance healing. Furthermore, it was reported that compared to mBC-SS, rBC-SS released more SS, which was shown to be due to the higher porosity of the rBC structure facilitating the impregnation of more SS. However, both materials exhibited rapid release of sufficient concentration of SS capable of enhancing the proliferation of cells involved in the wound healing process and collagen synthesis.

3.1 Effect of the biomaterials on wound closure

A macroscopic examination was carried out to determine the ability of the different dressings to improve the reduction of wound area and re-epithelialization. The photographs presented in Fig. 1 show the variation of a wounded area over time in all treatment groups. At D3, the wound healing rate was high in rBC (20.12 ± 5.03) and mBC (25.27 ± 1.6) groups compared to gauze (16.53 ± 6.18), with no significant difference. In rBC-SS2 (36.99 ± 0.66) and mBC-SS2 (29.20 ± 1.64) treatment groups, however, the wound area reduction rate was significantly higher compared to gauze. At D7 and D14, the healing rates were also higher in all other treated groups relative to gauze, except for the pristine BC group which showed significantly higher wound size reduction (as compared to the gauze group) only at D14 and not before. Interestingly enough, Jin *et al*.[29] reported that the healing rate in presence of gauze was higher than that with mBC; However, different wound models were employed in the two studies.

At each time point, the percentage of healing in presence of mBC was better than that with rBC, but the difference was not significant. This may be explained by the structured surface of mBC dressing. Visual observation indicates that over time, the healing rates in the presence of rBC-SS2 and mBC-SS2 composites were higher than those of rBC and mBC, respectively. The healing rate in the presence of mBC-SS1 at different time points was also higher than that in the presence of pure BC and gauze; by contrast, less difference was observed when compared with mBC-SS2. The reduction rate of wounded area in the presence of rBC-SS2 was higher than that of mBC-SS2 at D3, while at D7 and D14 the rate in the presence of the latter was the highest, though with no statistical difference. At D21, visual observation shows fully healed wounds in the different treatment groups; however, hair grew in the healed area only in mBC-SS2 group, showing complete healing. These observations demonstrate that mBC-SS2 could constitute an ideal material that can improve wound healing by reducing the wounded area.

3.2 Wound healing cascade upon biomaterial application

Tissue granulation is a crucial process in wound healing, and consists of the recruitment, proliferation, and differentiation of cells involved in healing, that is epithelial cells responsible for re-epithelialization, endothelial cells responsible for vascularization, fibroblasts that synthesize collagen (main

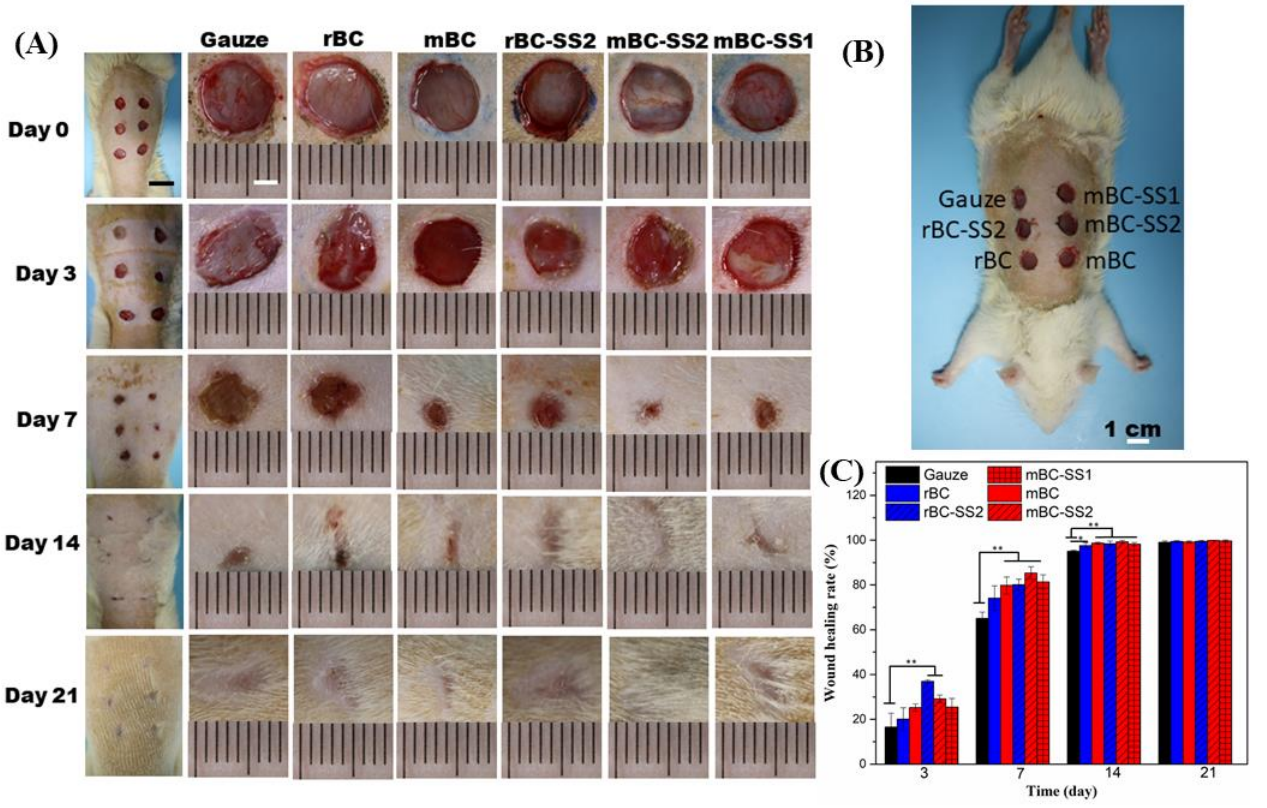

Fig. 1. (A) Macroscopic images of the wounds from different treatment groups. (B) Photo capture of a rat with the different treatment groups' positions. All images were under 10 mm magnification. (C) Variation of wound healing rate with time. Healing in presence of different treatment groups was faster compared to that with gauze. mBC-SS2 was the group that most accelerated healing (D7 and D14) with no statistical difference compared to rBC-SS2 and pure BC. The asterix (*) informs about the significant differences between the healing rates of the samples by comparison with gauze. (*) $P < 0,05$ and (**) $P < 0,01$.

skin ECM), and immune cells responsible for cleaning up the wound site and triggering the proliferation step. However, wound healing with excessive or chronic tissue granulation could result in the formation of fibrosis and scar; thereby, it is important to control tissue granulation. To understand the biological events and highlight the different actors involved in the wound healing process, histochemical staining was performed. Tissue samples were stained by H&E and the results are shown in Fig. 2. At D3 after surgery, the wounds treated with rBC and mBC presented granulated tissue which was not observed in gauze-covered wounds. Interestingly, all tested composites (rBC-SS2, mBC-SS1, and mBC-SS2) led to significantly thicker granulation tissue with infiltration of numerous inflammatory cells and fibroblasts as compared to rBC. Moreover, many blood vessels could be detected in the wounds protected by these composites, with lesser numbers in the mBC group. However, no blood vessels could be evidenced in the tissues from the rBC and gauze groups at this time point. Reportedly, neovascularization marks the proliferative phase of the wound healing process during which newly formed vessels provide oxygen and nutrients necessary for the growth of new tissue.[24,25] Hence, from the above results, it appears that in the composite materials, the presence of SS induces an early formation of granulation tissue by promoting the infiltration and proliferation of the different cells involved in the wound healing process, specifically fibroblasts, in agreement with the findings of our *in vitro* studies and other previously reported studies that emphasize the proliferative effect of SS during wound healing.[13,14,22,30] Additionally, the microgrooves of mBC on their own also facilitated the forming of the granulation tissue which was thicker in mBC than in rBC at D3. At D7, increased amounts of granulation tissue were observed in the different test groups as compared to the results observed on D3, probably due to the enhanced cell growth with time. In fact, during normal wound healing, the layer of granulation tissue always thickens during the proliferation phase before undergoing regression due to the differentiation of fibroblasts into myo-fibroblasts and the rearrangement of collagen *via* the cross-linking of its fibers.[2] In the current study, regression of neovascularization and rare infiltration of inflammatory cells occurred by D7 with mBC and its composites while remaining intense in the presence of rBC, rBC-SS2, and gauze. This indicates an early proliferation-remodeling phase transition by this time point (D7) when mBC and mBC-SS2 are applied, relative to the other dressing materials. At D14, with the exception of the gauze group, the thickness of the granulation tissue reduced significantly compared to D7. Glands and hair follicles could be observed in pristine BC groups, however, the rare presence of inflammatory cells and fibroblasts in mBC group at this

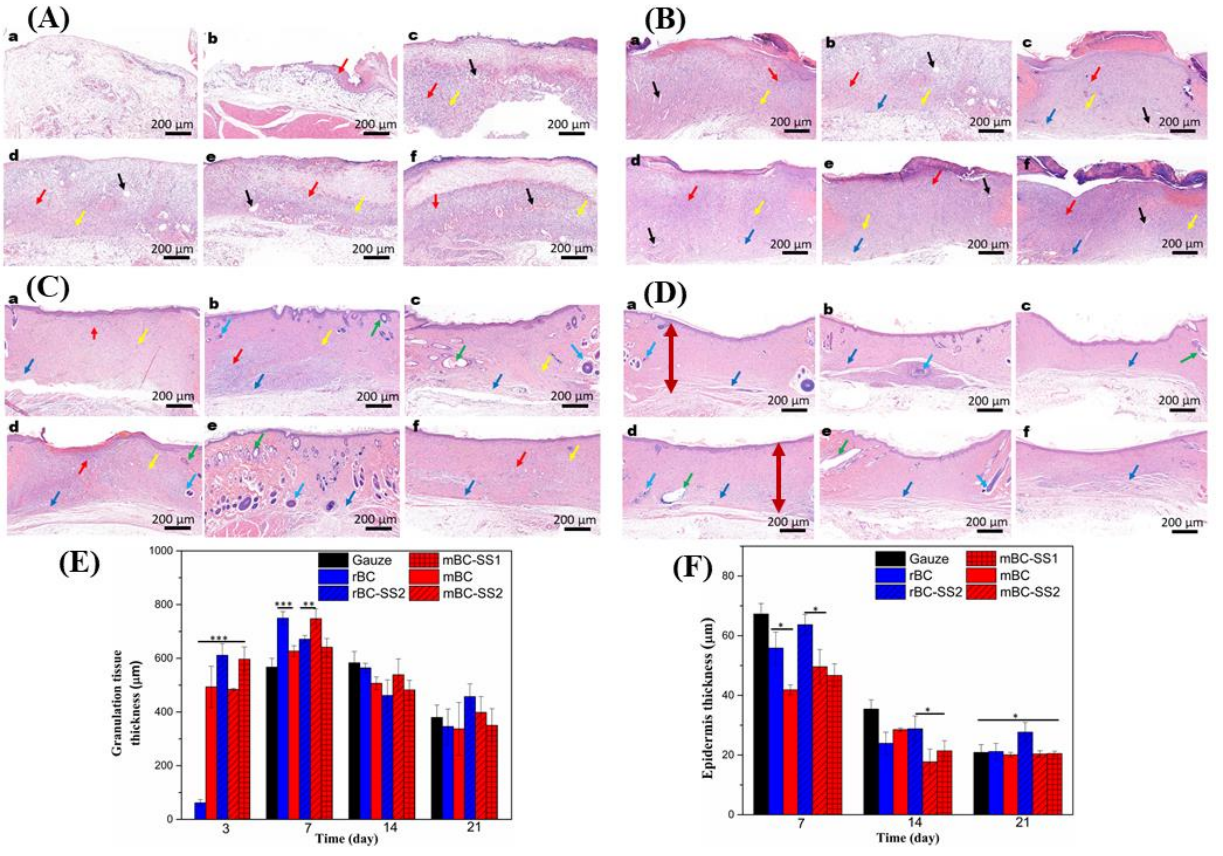

Fig. 2 HE-stained wound tissue sections viewed under a panoramic microscope at days 3 (A), 7 (B), 14 (C), and 21 (D) post-treatment, respectively. (E): Granulation tissue thickness, and (F): Epidermal thickness. Compared to that in the presence of pure BC and gauze, the granulation tissue in the presence of the composites was marked by early infiltration of inflammatory cells, fibroblasts, and angiogenesis which already regressed at D14. However, until D21, the neo-tissue was hypertrophied (red arrow) in the presence of rBC-SS2 and gauze compared to mBC-SS2 and other treatment groups. a: gauze, b: rBC c: mBC, d: rBC-SS2, e: mBC-SS2, f: mBC-SS1. (***) $P < 0.001$; (**) $P < 0.01$; (*) $P < 0.05$. (Arrows) black: blood vessels, blue: collagen fibers, yellow: fibroblast, red: inflammatory cells, green: hair follicles, and pale blue: glands.

time-point was contrasted with their higher numbers in the rBC group. This suggests an initiation of the remodeling phase in presence of mBC while rBC-dressed wounds were just transitioning from proliferation to remodeling. The latter was more advanced in the composites, with more glands, hair follicles, and the absence of fibroblasts and inflammatory cells in the mBC-SS2 group compared to the mBC-SS1, and then mBC, respectively. Thus by D14, there is the regression of granulation tissue in the different treatment groups, more precisely those of mBC and mBC-SS2 in the remodeling stage, whereas the rBC and rBC-SS2 groups transition from proliferation to remodeling stage. At D21, the newly formed tissue was significantly less thick in BC alone, mBC-SS1, and mBC-SS2 compared to D14; whereas the thickness in rBC-SS2 at these two-time points was similar. Hence, we deduce that among the different tested materials, mBC-SS2 prevents the hypertrophy of the neo-tissue. Thus, mBC-SS2 would be the best dressing to promote accelerated skin tissue repair without tissue hypertrophy.

Wound re-epithelialization was observed on D7 in all groups; however, the entire wound area was not re-epithelialized. At D14 and D21, the wound area of the different dressings was entirely covered by the epidermis, with reduced layer thickness as compared to D7. This corroborates the above results, with active cell (keratinocytes) proliferation responsible for thicker tissue layers at D7, followed by a reduction in tissue size (D14 and D21) due to maturation which in the specific case of epithelialization corresponds to the differentiation of keratinocytes into corneocytes that restore the normal thickness of the epidermis.[2]

Masson's trichrome staining was further performed to assess the alignment and volume fraction deposition of collagen, and the organization of fibroblast architecture (Fig. 3). Collagen volume fraction increased over time and regressed after peaking in all treatment groups. At D3 and D7, the amount of collagen deposition was significantly higher in rBC-SS2 and mBC-SS2 compared to rBC and mBC, respectively. This is in accordance with the *in vitro* and other studies which state that SS enhances the synthesis of collagen.[15,31] The amount of collagen synthesis in the presence of rBC-SS2 was higher than that in the presence of mBC-SS2, with a significant difference at D3. This also confirms our *in vitro* test results and could be explained by the high quantity of SS uptake, which is facilitated by the porosity

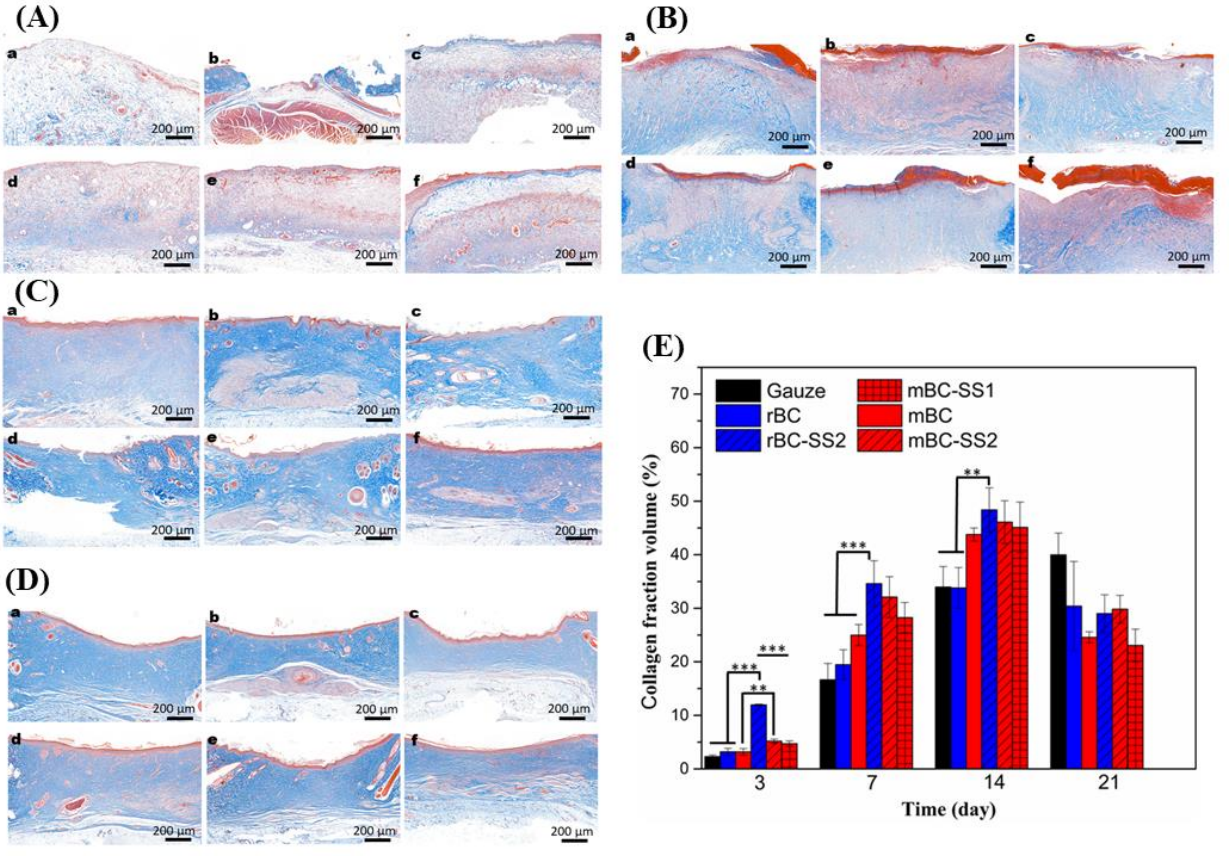

Fig. 3 Masson's trichrome-stained wound tissue sections viewed under a panoramic microscope at days 3 (A), 7 (B), 14 (C), and 21 (D) post-treatment, respectively. (E) Collagen fraction volume at various times. Collagen (blue color) was significantly synthesized in the presence of composites compared to pure BC and gauze. Moreover, the collagen distribution was uniform and homogeneous in the presence of mBC and its composites while random collagen fibers with non-uniform distribution were observed in the presence of rBC and its composites. a: gauze, b: rBC c: mBC, d: rBC-SS2, e: mBC-SS2, f: mBC-SS1 (***) $P < 0.001$; (**) $P < 0.01$.

of rBC. It has been reported that collagen is responsible for the strength and integrity of tissue matrix;[25] thereby, it could be speculated that rBC-SS2 and mBC-SS2 would be the best biomaterials that can provide strength to regenerated skin tissue. However, it has been shown that the anarchic deposition of collagen leads to the formation of fibrosis and dense scar tissue.[32] At D7 and D14, we observed a homogeneous distribution and a uniform layer of collagen in the mBC group and its composites whereas the distribution was random and non-homogeneous in the wounds from the groups of rBC and its composites. Fibroblasts being responsible for the synthesis of collagen, it thus appears that mBC and its composites induce the orderly, homogeneous, and uniform alignment of fibroblasts whereas the latter are randomly and non-homogeneously distributed in rBC and its composites-treated wounds. Hence, mBC-SS2 would constitute the ideal dressing, capable of enhancing the synthesis of collagen and inducing its homogeneous and uniform deposition in order to promote the regeneration of skin as in normal tissue and to avoid the formation of fibrosis and scar. At D21, the amount of collagen was reduced compared to the D14 in the different treatment groups, which could be explained by the rearrangement and differentiation of collagen.

3.3 Molecular expression under biomaterial treatment

To further elucidate the molecular process involved in wound healing upon the use of the different dressing materials, immunohistochemical staining was performed to assess the effect of different samples on re-epithelialization, wound contraction, and angiogenesis. For this purpose, CK-14, VEGF, Col-I, Coll-III, and α-SMA were stained, which represent characteristic markers of the different layers of the skin and whose expression thus determines the different stages of wound healing. Figs. 4-6 show the expression of the different markers in the wounds after D7 and D14 of treatment with the different dressings.

Re-epithelialization is a critical and urgent part of the wound healing process in that it helps restore the skin's role as a physical barrier and prevent the body from being exposed to harmful substances.[23] CK-14 is a marker for the proliferation of keratinocytes and is expressed in the basal layer of the epidermis and in hair, its expression was determined to evaluate the re-epithelialization of the wounds.[6] At D7 of post-wounding and treatment with different dressings, CK-14 was expressed in the presence of all samples including gauze, rBC, mBC, rBC-SS2, and mBC-SS2; however, it did not cover the entire wound surface. The CK-14 layer was thicker with the composites, especially mBC-SS2, suggesting the

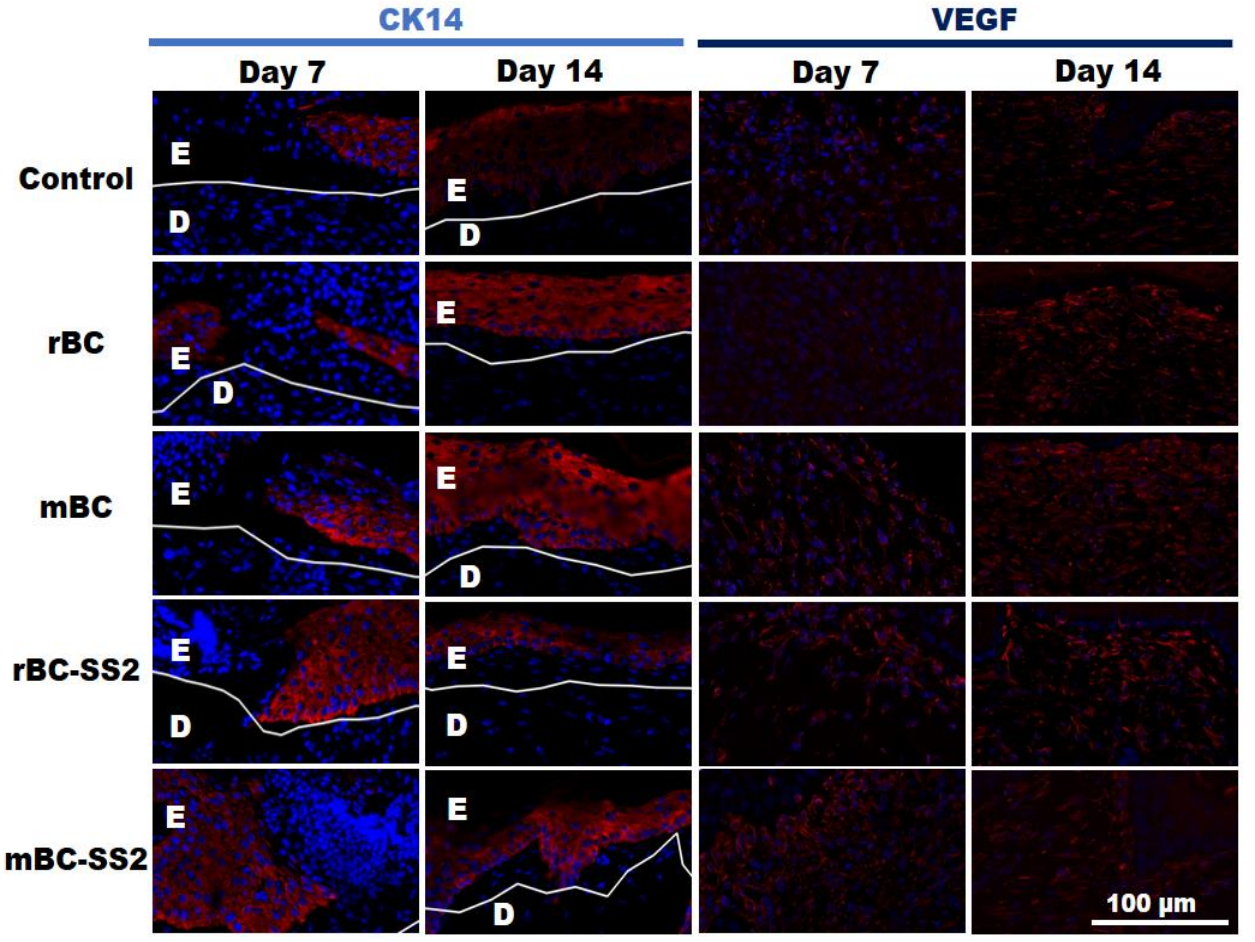

Fig. 4 Images of immunohistochemically stained wound tissue sections viewed under a panoramic microscope at days 7 and 14 post-treatment. CK-14 and VEGF were stained and observed under 100 µm magnification. At D14, the wound was re-epithelialized in all treatment groups with CK-14 marking the differentiation of keratinocytes with the composites, whereas these cells were in the active phase of proliferation in the presence of pure BC and gauze. Furthermore, at D14, VEGF synthesis regressed in the presence of mBC-SS2 (angiogenesis regression) while it was still active in the other treatment groups. E and D correspond to the epidermis and dermis layers, respectively. Nucleus stained blue, and specific markers-stained red.

improvement in the proliferation of keratinocytes by rBC-SS2 and mBC-SS2 composites.[14,22] By D14, the CK-14 layer covered the entire surface of the wounds, and was thicker in the gauze, rBC, and mBC groups compared to the composites in which the thickness had regressed. This is in adequacy with the findings of the histological analysis; the thicker CK-14 layer observed in the gauze and pure BC groups at this time point indicates the proliferation stage which was already terminated in the other groups (composites) where the expression of CK-14 had regressed as a consequence of the maturation of the keratinocytes indicating an ongoing wound healing remodeling phase.[6]

As another determining element in the genesis of the dermis in the skin, wound contraction was explored. Fibroblasts constitute the motor cells of wound contraction; they are activated after wounding, proliferate, and differentiate into myofibroblasts expressing α-SMA.[2,29,33–36] Besides, α-SMA is also expressed in smooth muscle cells, constituents of blood vessels.[37] The protein marker was thus stained as a measure of myofibroblast density and angiogenesis. At D7, the level of expressed α-SMA was higher in the presence of the composites (with the highest level in mBC-SS2) compared to mBC, rBC, and gauze, respectively, signifying a well-advanced proliferation phase in the composites groups with the presence of myofibroblasts and high angiogenesis. This confirms the potential of SS to enhance angiogenesis and fibroblast proliferation as reported by other studies.[14,38–40] However, at D14, the rate of α-SMA expression regressed in the presence of all samples. This declination could be explained by the regression of angiogenesis and apoptosis of myofibroblasts during the remodeling step. VEGF, a protein expressed by endothelial cells was further stained to confirm the degree of angiogenesis estimated by the result of α-SMA expression. As expected, the expression of VEGF aligned with that of α-SMA. Overall, mBC-SS2 outstood the other dressing materials, orchestrating a wound-healing cascade ahead of that in the other experimental groups.

Col-III, the predominant ECM protein in wound contraction[2] which is gradually replaced by Col-I (determines the strength of the skin) was also examined along with Col-I.

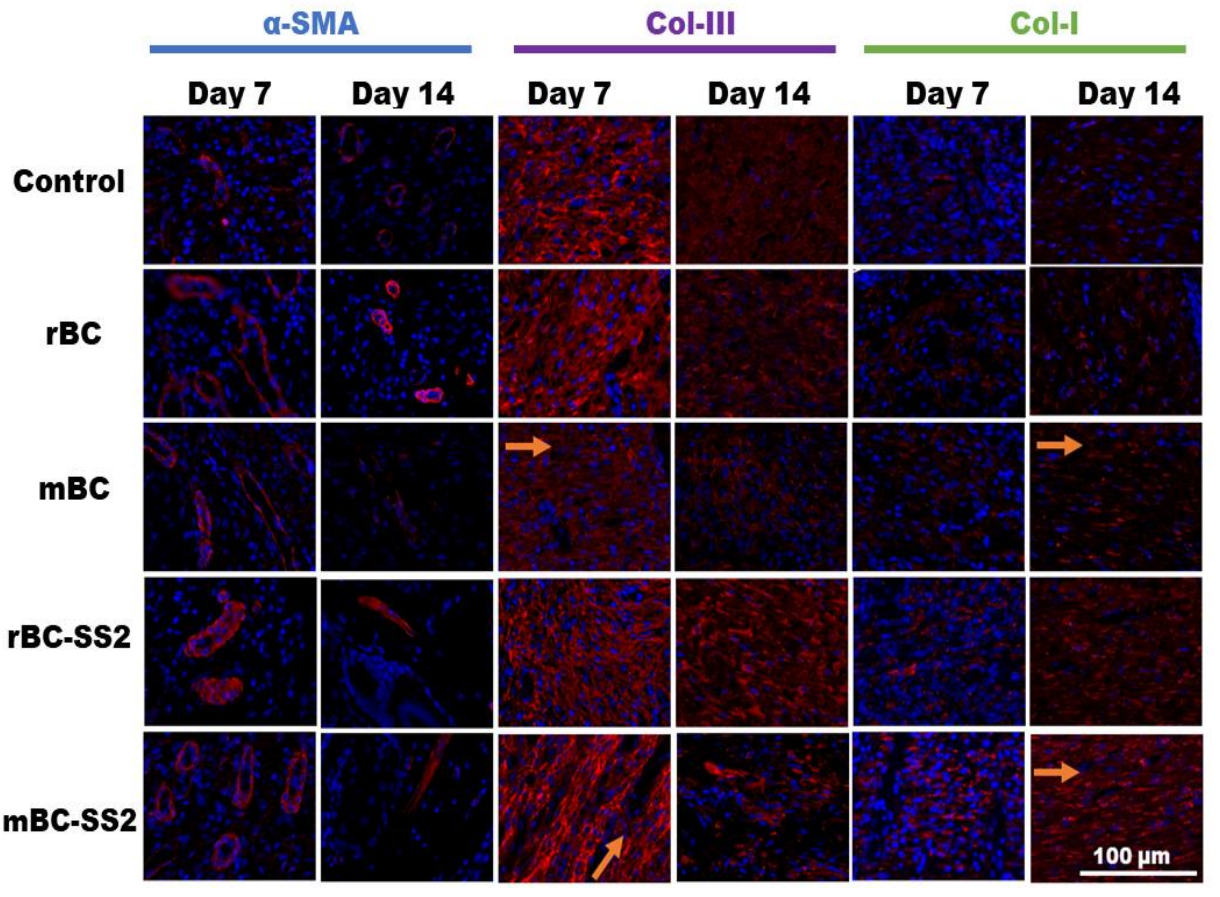

Fig. 5 Images of immunohistochemically stained wound tissue sections viewed under a panoramic microscope at days 7 and 14 post-treatment. α-SMA, Col-I, and Col-III were stained and observed under 100 µm magnification. At D14, Col-III regressed and was replaced by Col-I in the presence of mBC-SS2 while both types of collagen were dense in rBC-SS2 and only Col-III was still intense in pure BC and gauze. Moreover, the collagens were deposited according to the orientation of mBC and its composites. Arrows indicate the orientation of collagen deposition. Nucleus stained blue, and other specific markers-stained red.

At D7, the expression of Col-III in the composites groups was significantly higher compared to that in the presence of gauze and pure BC. The result is also consistent with that of histology and confirms the potential of SS to improve collagen synthesis. However, the amount of Col-III expression was higher than that of Col-I with all samples, which is in accordance with the results reported in other works,[2,6] and could be explained by the fact that Col-III is most expressed during the proliferation stage and is replaced by Col-I during remodeling. Thereby, healing in the presence of the different samples was at the proliferation stage, most active with the composites. At D14, the level of Col-III expression was still high in the presence of rBC-SS2 compared to that in the presence of gauze and pure BC while this expression considerably regressed in the presence of mBC-SS. By contrast, the level of Col-I expression in the presence of the latter was significantly higher than in the presence of rBC-SS2, pure BC, and gauze, respectively. Moreover, by D14, the amount of Col-I expression was significantly higher compared to that of D7 in the presence of all the treatment groups, especially mBC-SS2; this can also be explained by the conversion of Col-III to Col-I during the transition of proliferation to the remodeling step. This shows that at D14, healing in the presence of mBC-SS2 was at the remodeling stage while the other treatment groups were still in the proliferation phase. The high Col-III expression amount of up to D14 in the presence of rBC-SS2 could also be explained by excessive wound contraction which has been reported as a source of fibrosis,[25,29] Moreover, as indicated by arrows in the figures, the collagen fibers including Col-I and Col-III were aligned according to the microgroove orientation of mBC and its composites while their organization had no such architecture in the presence of rBC and its composites. The formation of fibrosis and scar is caused by the anarchic deposition of collagen, the findings confirm the hypothesis in our previous studies[26] and would be of great importance in avoiding the genesis of fibrosis.

4. Conclusion

According to our previous studies,[26,27] BC-SS composites enhance the proliferation of fibroblast and keratinocyte cells while mBC and its composites exhibit improved mechanical properties relative to rBC and its composites. The current study evaluated these biomaterials *in vivo* and compared their

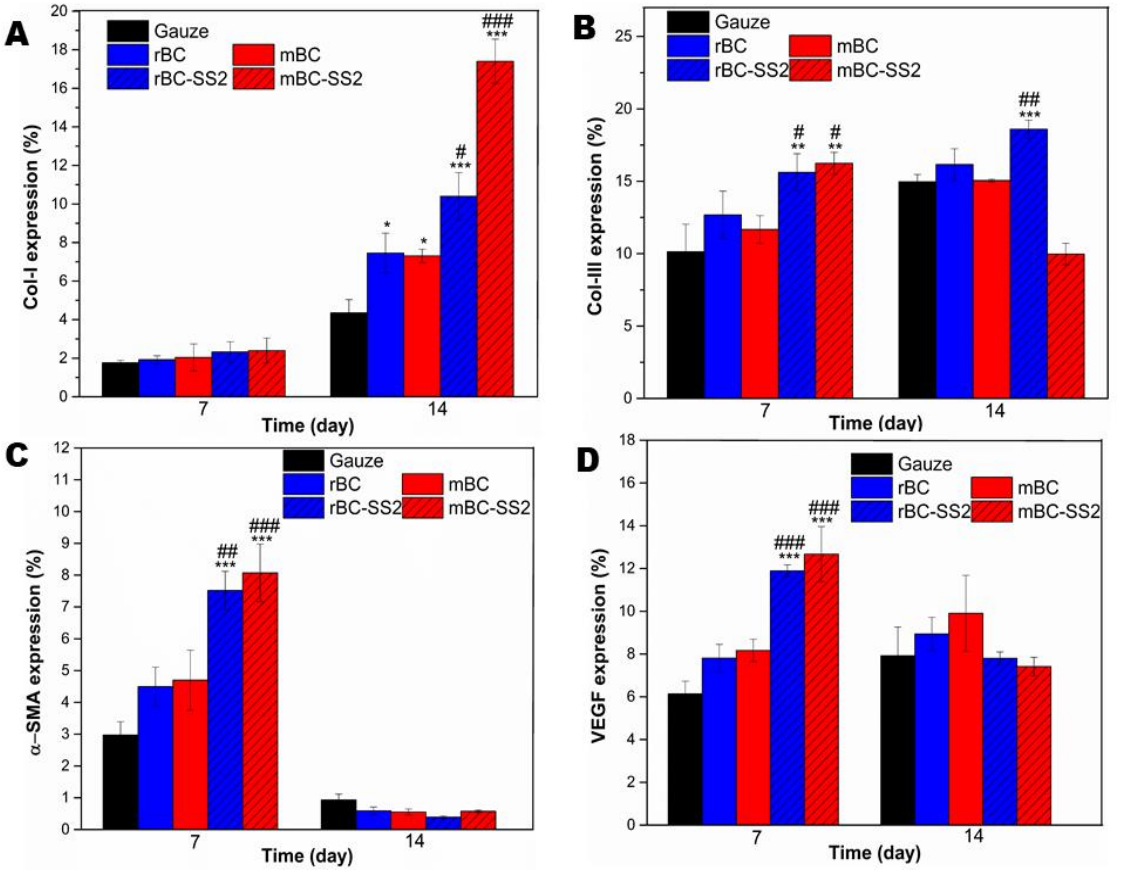

Fig. 6 Expression rate of Col-I (A), Col-III (B), α-SMA (C), and VEGF (D) for different treatment groups on different days. (***/###) $P < 0.001$; (**/##) $P < 0.01$; (*/#) $P < 0.05$; (*): comparison between gauze and BC composites; (#): comparison between pure BC and BC composites.

effects on the wound healing process and its result. Macroscopically, wound healing was faster in the presence of BC-SS2 composites whereas histologically, these composites had induced very early recruitment and proliferation of inflammatory cells, fibroblasts, and keratinocytes which differentiated and led to the regression of wound contraction at D14. By contrast, the recruitment of these cells was late, and their proliferation was still active until D14 in the presence of pure BC and gauze. The current study demonstrates *in vivo* that the application of BC-SS2 composites as wound dressings improves wound healing compared to pure BC. Thereby, there is confirmation of the potential of SS to enhance wound healing. Furthermore, compared to rBC-SS2, mBC-SS2 renders faster healing, induces homogeneous distribution of fibroblasts and collagen deposition, and inhibits neo-tissue hypertrophy. Moreover, the wound contraction is less excessive in presence of mBC-SS2 than with rBC-SS2, which would prevent fibrosis and the formation of scars.

We conclude from the present study that mBC-SS2 represents the best dressing for inducing rapid wound re-epithelialization, angiogenesis, and wound contraction with less risk of generating the formation of fibrosis and scar.

Conflict of Interest

The authors declare no conflict of interest.

Supporting information

Applicable.

Abbreviations

BC: bacterial cellulose; SS: silk sericin; mBC: microstructured bacterial cellulose; rBC: random bacterial cellulose; PDMS: poly(dimethylsiloxane); D: day; HR: healing rate; Cv: collagen volume; Ca: collagen area; Ta: total tissue area; CK-14: cytokeratin 14; VEGF: vascular endothelial growth factor; Col-I: collagen I; Col-III: collagen III; α-SMA: α-smooth muscle actin

Reference

[1] E. Altun, M. O. Aydogdu, F. Koc, M. Crabbe-Mann, F. Brako, R. Kaur-Matharu, G. Ozen, S. E. Kuruca, U. Edirisinghe, O. Gunduz, M. Edirisinghe, *Macromolecular Materials and Engineering*, 2018, **303**, 1870010, doi: 10.1002/mame.201870010.

[2] E. Y. X. Loh, N. Mohamad, M. B. Fauzi, M. H. Ng, S. F. Ng, M. C. I. Mohd Amin, *Scientific Reports*, 2018, **8**, 2875, doi: 10.1038/s41598-018-21174-7.

[3] J. Ahmed, M. Gultekinoglu, M. Edirisinghe, *Biotechnology Advances*, 2020, **41**, 107549, doi: 10.1016/j.biotechadv.2020.107549.

[4] M. O. Aydogdu, E. Altun, M. Crabbe-Mann, F. Brako, F. Koc,

G. Ozen, S. E. Kuruca, U. Edirisinghe, C. J. Luo, O. Gunduz, M. Edirisinghe, *International Wound Journal*, 2018, **15**, 789-797, doi: 10.1111/iwj.12929.
[5] J. Chen, Y. Zhan, Y. Wang, D. Han, B. Tao, Z. Luo, S. Ma, Q. Wang, X. Li, L. Fan, C. Li, H. Deng, F. Cao, *Acta Biomaterialia*, 2018, **80**, 154-168, doi: 10.1016/j.actbio.2018.09.013.
[6] N. Mohamad, E. Y. X. Loh, M. B. Fauzi, M. H. Ng, M. C. I. Mohd Amin, *Drug Delivery and Translational Research*, 2019, **9**, 444-452, doi: 10.1007/s13346-017-0475-3.
[7] P. Kotcharat, P. Chuysinuan, T. Thanyacharoen, S. Techasakul, S. Ummartyotin, *Sustainable Chemistry and Pharmacy*, 2021, **20**, 100404, doi: 10.1016/j.scp.2021.100404.
[8] A. Gupta, S. M. Briffa, S. Swingler, H. Gibson, V. Kannappan, G. Adamus, M. Kowalczuk, C. Martin, I. Radecka, *Biomacromolecules*, 2020, **21**, 1802-1811, doi: 10.1021/acs.biomac.9b01724.
[9] Z. Luo, J. Liu, H. Lin, X. Ren, H. Tian, Y. Liang, W. Wang, Y. Wang, M. Yin, Y. Huang, J. Zhang, *International Journal of Nanomedicine*, 2020, **15**, 1-15, doi: 10.2147/ijn.s231556.
[10] A. Escobar, M. Perez, G. Romanelli, G. Blustein, *Arabian Journal of Chemistry*, 2020, **13**, 9243-9269, doi: 10.1016/j.arabjc.2020.11.009.
[11] M. O. Aydogdu, E. Altun, J. Ahmed, O. Gunduz, M. Edirisinghe, *Polymers*, 2019, **11**, 1148, doi: 10.3390/polym11071148.
[12] M. E. Cam, M. Crabbe-Mann, H. Alenezi, A. N. Hazar-Yavuz, B. Ertas, C. Ekentok, G. S. Ozcan, F. Topal, E. Guler, Y. Yazir, M. Parhizkar, M. Edirisinghe, *European Polymer Journal*, 2020, **134**, 109844, doi: 10.1016/j.eurpolymj.2020.109844.
[13] S. Napavichayanun, R. Yamdech, P. Aramwit, *International Journal of Polymeric Materials and Polymeric Biomaterials*, 2018, **67**, 61-67, doi: 10.1080/00914037.2017.1297943.
[14] P. Aramwit, S. Palapinyo, T. Srichana, S. Chottanapund, P. Muangman, *Archives of Dermatological Research*, 2013, **305**, 585-594, doi: 10.1007/s00403-013-1371-4.
[15] P. Aramwit, T. Siritienthong, T. Srichana, J. Ratanavaraporn, *Cells Tissues Organs*, 2013, **197**, 224-238, doi: 10.1159/000345600.
[16] G. Cheng, Z. Davoudi, X. Xing, X. Yu, X. Cheng, Z. Li, H. Deng, Q. Wang, *ACS Biomaterials Science & Engineering*, 2018, **4**, 2704-2715, doi: 10.1021/acsbiomaterials.8b00150.
[17] S. Baptista-Silva, S. Borges, A. R. Costa-Pinto, R. Costa, M. Amorim, J. R. Dias, Ó. Ramos, P. Alves, P. L. Granja, R. Soares, M. Pintado, A. L. Oliveira, *ACS Biomaterials Science & Engineering*, 2021, **7**, 1573-1586, doi: 10.1021/acsbiomaterials.0c01745.
[18] E. M. El-Fakharany, G. M. Abu-Elreesh, E. A. Kamoun, S. Zaki, D. A. Abd-EL-Haleem, *RSC Advances*, 2020, **10**, 5098-5107, doi: 10.1039/c9ra09419a.
[19] L. Lamboni, M. Gauthier, G. Yang, Q. Wang, *Biotechnology Advances*, 2015, **33**, 1855-1867, doi: 10.1016/j.biotechadv.2015.10.014.
[20] J. Nam, Y. Hyun, S. Oh, J. Park, H.-J. Jin, H. W. Kwak, *Polymer Testing*, 2021, **97**, 107161, doi: 10.1016/j.polymertesting.2021.107161.
[21] Y. Cheng, G. Cheng, C. Xie, C. Yin, X. Dong, Z. Li, X. Zhou, Q. Wang, H. Deng, Z. Li, *Advanced Healthcare Materials*, 2021, **10**, 2001646, doi: 10.1002/adhm.202001646.
[22] L. Lamboni, Y. Li, J. Liu, G. Yang, Biomacromolecules, 2016, **17**, 3076-3084, doi: 10.1021/acs.biomac.6b00995.
[23] S. Osseiran, J. D. Cruz, S. Jeong, H. Wang, C. Fthenakis, C. L. Evans, *Biomedical Optics Express*, 2018, **9**, 6425, doi: 10.1364/boe.9.006425.
[24] P. R. F. de Sousa Moraes, S. Saska, H. Barud, L. R. de Lima, V. da Conceição Amaro Martins, A. M. de Guzzi Plepis, S. J. L. Ribeiro, A. M. M. Gaspar, *Materials Research*, 2016, **19**, 106-116, doi: 10.1590/1980-5373-mr-2015-0249.
[25] B. O. Ode Boni, L. Lamboni, T. Souho, M. Gauthier, G. Yang, *Materials Horizons*, 2019, **6**, 1122-1137, doi: 10.1039/c9mh00291j.
[26] B. O. O. Boni, L. Lamboni, B. M. Bakadia, S. A. Hussein, G. Yang, *Engineered Science*, 2020, **10**, 68-77, doi: 10.30919/es8d906.
[27] L. Lamboni, C. Xu, J. Clasohm, J. Yang, M. Saumer, K.-H. Schäfer, G. Yang, *Materials Science and Engineering: C*, 2019, **102**, 502-510, doi: 10.1016/j.msec.2019.04.043.
[28] P. Aramwit, N. Bang, *BMC Biotechnology*, 2014, **14**, 104, doi: 10.1186/s12896-014-0104-
[29] M. Jin, W. Chen, Z. Li, Y. Zhang, M. Zhang, S. Chen, *Cellulose*, 2018, **25**, 6705-6717, doi: 10.1007/s10570-018-2041-7.
[30] S. Napavichayanun, R. Yamdech, P. Aramwit, *Archives of Dermatological Research*, 2016, **308**, 123-132, doi: 10.1007/s00403-016-1621-3.
[31] P. Aramwit, S. Kanokpanont, W. De-Eknamkul, K. Kamei, T. Srichana, *Journal of Biomaterials Science, Polymer Edition*, 2009, **20**, 1295-1306, doi: 10.1163/156856209x453006.
[32] D. D. Lo, A. S. Zimmermann, A. Nauta, M. T. Longaker, H. P. Lorenz, *Birth Defects Research Part C: Embryo Today: Reviews*, 2012, **96**, 237-247, doi: 10.1002/bdrc.21018.
[33] Y. Lu, Y. Wang, J. Zhang, X. Hu, Z. Yang, Y. Guo, Y. *Acta Biomaterialia*, 2019, **89**, 217-226, doi: 10.1016/j.actbio.2019.03.018.
[34] B. Hinz, G. Celetta, J. J. Tomasek, G. Gabbiani, C. Chaponnier, *Molecular Biology of the Cell*, 2001, **12**, 2730-2741, doi: 10.1091/mbc.12.9.2730.
[35] Y. Li, S. Wang, R. Huang, Z. Huang, B. Hu, W. Zheng, G. Yang, X. Jiang, *Biomacromolecules*, 2015, **16**, 780-789, doi: 10.1021/bm501680s.
[36] D. Zmejkoski, D. Spasojević, I. Orlovska, N. Kozyrovska, M. Soković, J. Glamočlija, S. Dmitrović, B. Matović, N. Tasić, V. Maksimović, M. Sosnin, K. Radotić, *International Journal of Biological Macromolecules*, 2018, **118**, 494–503, doi: 10.1016/j.ijbiomac.2018.06.067.
[37] L. Cheng, Z. Cai, T. Ye, X. Yu, Z. Chen, Y. Yan, J. Qi, L. Wang, Z. Liu, W. Cui, L. Deng, *Advanced Functional Materials*, 2020, **30**, 2001196, doi: 10.1002/adfm.202001196.
[38] T. Siritientong, A. Angspatt, J. Ratanavaraporn, P. Aramwit, *Pharmaceutical Research*, 2014, **31**, 104-116, doi: 10.1007/s11095-013-1136-y.

[39] Y. Y. Jo, D. W. Kim, J. Y. Choi, S. G. Kim, *Scientific reports*, 2019, **9**, 1–11, doi: 10.1038/s41598-019-40027-5.
[40] S. Kanokpanont, S. Damrongsakkul, J. Ratanavaraporn, P. Aramwit, *International Journal of Pharmaceutics*, 2012, **436**, 141-153, doi: 10.1016/j.ijpharm.2012.06.046.

Author Information

Dr. Biaou Oscar Ode Boni *is currently a postdoctoral fellow at Huazhong University of Science and Technology (China) in the laboratory of Prof. Guang Yang. He carried out his Ph.D. studies (2016–2020) at the School of Life Science of the same university in biochemistry and molecular biology. He received his master's (2012) and bachelor's (2009) degrees from the University of Abomey-Calavi (Benin) in biochemistry and molecular biology. His research interests include the immune response to biomaterials and the development of biomaterials for vascular graft, nerve conduit, and wound healing applications.*

Lallepak Lamboni *is a PhD in Biomedical Engineering. She carried out a postdoctoral fellowship (2016-2019) at Huazhong University of Science and Technology (China) in the department of Biomedical Engineering, under the supervision of Prof Guang Yang with whom she also studied for her PhD degree (2016), building upon a B.Sc. degree (2011) in Biology and Health from the Faculty of Science and Technology of Fez in Morocco. She has worked in tissue engineering and regenerative medicine, with research interests including the development of biomimetic materials for tissue repair and regeneration, the study of cell-biomaterial interactions, and the functional exploration of biomacromolecules.*

Dr. Lin Mao *is currently a lecturer in the College of Life Science, Henan Agricultural University. She received her Master's degree in Biochemistry and Molecular Biology from Huazhong Normal University (2015), and PhD degree in Biopharmaceutical Engineering from Huazhong University of Science and Technology, in the laboratory of Prof. Guang Yang (2021). Her research interests focus on biological effects of multifunctional nanobiomaterials and their biomedical applications; and the development of electroactive biomaterials for tissue engineering and regenerative medicine, in addition, her research interest involve the exploration of antiviral effect and mechanism of nanomaterials.*

Bianza Moise Bakadia *is currently a Ph.D. student at Huazhong University of Science and Technology. He received a Bachelor of Science degree from the Higher Institute of Medical Techniques of Lubumbashi, DR. Congo, and a Master's degree from Huazhong University of Science and Technology, China. His research interests include biomedical analysis of biological fluids, the immune response to microorganisms, and the development of biomaterials for tissue engineering. He has published more than 15 SCI papers.*

Dr. Zhijun Shi *is a lecturer in Department of Biomedical Engineering, School of Life Science and Technology, Huazhong University of Science and Technology, Wuhan, P.R.China. He received his BS and PhD degrees in Biotechnology and Microbiology in 2008 and 2014, respectively from Huazhong University of Science and Technology, PR China. He has authored more than 30 publications in high impact international peer-reviewed journals, edited 1 books, authored several chapters, and registered more than 10 authorized patents. His research interests include biofabrication based on microbes and fabrication of functional hydrogels based on natural polymers.*

Dr. Guang Yang *is Professor at Huazhong University of Science and Technology, China. She received PhD degree in Chemistry from Wuhan University, China. She remained the Distinguished Young Chutian Scholar and Outstanding Talents in Hubei province, as well as Alexander von Humboldt and JSPS fellow. She was also a visiting scholar in Asahi Chemical Industry Co., Ltd., Japan and University of Akron, USA. Currently, she is serving as the Deputy Director of the Cellulose division of the Chinese Chemical Society, Deputy Director of the Polymer Characterization Committee of the Chinese Chemical Society, and the council member of several committees, including the Nanocellulose and Materials Committee of China Paper Association, the Biomedical Polymer Materials Branch of China Biomaterials Society. She has authored more than 160 publications in high impact international peer-reviewed journals, edited 3 books, authored several book chapters, and registered more than 20 authorized patents. Her current research focuses on the development of nanocellulose-based functional materials, design and fabrication of novel nano-drug transporters, 3D printing, nano-assembly of ordered materials, and tissue engineering*